

Primljen / Received: 23.1.2018.

Ispravljen / Corrected: 10.5.2018.

Prihvaćen / Accepted: 24.6.2018.

Dostupno online / Available online: 10.10.2020.

# Simulation of Scour at Bridge Supports

## Authors:



Assoc.Prof. **Yasser Moussa**, PhD. CE  
Jazan University, KSA, Saudi Arabia  
Department of of Civil Engineering  
[ymoussa@jazanu.edu.sa](mailto:ymoussa@jazanu.edu.sa)

Corresponding author



Assist.Prof. **Mahoud Atta**, PhD. CE  
Jazan University, KSA, Saudi Arabia  
Mechanical Engineering Departement  
[mibrahim@jazanu.edu.sa](mailto:mibrahim@jazanu.edu.sa)

Research Paper

**Yasser Moussa, Mahoud Atta**

## Simulation of Scour at Bridge Supports

Groups of piers are used on bridges to minimise scour around bridge supports. The prediction of scour around piers due to interaction of vortices around bridge piers is more complex compared to scour prediction around a single pier. Four arrangements of bridge piers with different spaces in the lateral and longitudinal directions are investigated under clear water conditions to observe scour generation around bridge foundations. The experimental study is performed in a rectangular open channel. A 3D numerical study based on fluid dynamics is also conducted. Results show that different pier group arrangements produce smaller scour holes than a single pier.

### Key words:

local scour, hydraulic structure, piers, group of piles, SSIM

Prethodno priopćenje

**Yasser Moussa, Mahoud Atta**

## Simulacija podlokavanja na potpornjima mostova

Na mostovima se koriste skupine stupova kako bi se na minimum svelo podlokavanje oko potpornih elemenata. Predviđanje podlokavanja oko stupova uslijed interakcije vrtloga oko stupova mosta složenije je od predviđanja podlokavanja na pojedinačnim stupovima. U radu se istražuju četiri rasporeda stupova s različitim razmacima u bočnom i uzdužnom smjeru kako bi se analizirala pojava vrtloga oko temelja mosta u uvjetima bistrice vode. Provedeno je eksperimentalno ispitivanje u pravokutnom otvorenom kanalu i trodimenzionalno numeričko ispitivanje bazirano na dinamici fluida. Rezultati pokazuju da se u raznim rasporedima stupova postižu manje dubine podlokavanje nego što je to slučaj kod samo jednog stupa.

### Ključne riječi:

lokalno podlokavanje, hidraulička građevina, stupovi, skupina pilota, SSIM

Vorherige Mitteilung

**Yasser Moussa, Mahoud Atta**

## Simulation der Unterwaschung von Brückenträgern

Bei Brücken werden Pfeilergruppen verwendet, um die Unterwaschung um die Stützelemente herum zu minimieren. Die Vorhersage der Unterwaschung um Säulen aufgrund von Wirbelwechselwirkungen um Brückenpfeiler ist komplexer als die Vorhersage der Unterwaschung einzelner Pfeiler. Die Arbeit untersucht vier Pfeileranordnungen mit unterschiedlichen Abständen in Seiten- und Längsrichtung, um das Auftreten von Wirbeln um das Brückenfundament bei klarem Wasser zu analysieren. Eine experimentelle Prüfung in einem rechteckigen offenen Kanal und eine dreidimensionale numerische Prüfung basierend auf der Fluidodynamik wurden durchgeführt. Die Ergebnisse zeigen, dass bei verschiedenen Pfeileranordnungen eine geringere Tiefe erreicht wird als bei nur einem Pfeiler.

### Schlüsselwörter:

lokale Unterwaschung, hydraulische Struktur, Pfeiler, Pfahlgruppe, SSIM

### 1. Introduction

Excessive scour around bridge supports can increase settlement of foundations and cause damage to bridge piers and abutments. More than 1400 bridges were destroyed in the United State from 1996 to 2005 because of scour problem [1]. Scour refers to the removal of bed and/or bank materials because of the erosive action of flow [2]. Generally, the scour around bridge piers can be classified into three types: general scour, contraction scour, and local scour. General scour represents the degradation and aggradation of river bed [3]. Contraction scour results from the decrease in the channel cross-sectional area. This type of scour occurs because of the construction of hydraulic structures along the waterway [4]. Local scour occurs at the bridge foundation. Two types of local scour exist: clear-water scour and live-bed scour. The scour at the bridge foundation is a dynamic process and varies with the flow characteristics and shape, and with the arrangement of piers and abutments of bridges [5].

Groups of piles are widely used as a foundation to support river and marine structures. The scour around these piles can represent danger by reducing the bridge capacity to resist loads [6]. Atilla and Magnus Larson (2000) [7] investigated the field data from the Pacific Coast of Japan for scour around a group of piles under the effect of oscillating waves and found that the scour hole width has a minor correlation with the Keulegan–Carpenter number. Many researchers have investigated and analysed the scour formation at a single bridge pier [8-12]. Richardson and Davis (2001) [13] predicted equation HEC-18 for estimating the local scour depth at a single pile. However, reviews of studies of scour at groups of piles are limited [14-17].

Sumer et al. (2005) [18] reported that the scour around different arrangements of pile groups occurred in the form of a saucer-shaped depression. Amini et al. (2012) [16] estimated the local scour depth at pile groups for shallow flow conditions. Various methods were evaluated to estimate the local scour depth at groups of piles [19]. The scour around eight different pile arrangement models was investigated numerically and experimentally [17].

The lateral and longitudinal spacing between piles were constant. Furthermore, the depth of scour decreased by 42 % for tandem arrangements of piles compared to the depth of scour for a single pile. Computational fluid dynamic models were used to simulate scour around bridge piers and abutments [12, 17, 20-22]. The present paper aims to clarify experimentally and numerically the effect of varying lateral and longitudinal spacing between bridge piers on the scour formed at the bridge foundation.

### 2. Experimental work

The experimental work was carried out in a re-circulating rectangular open channel. The experimental apparatus consists of two flumes: the lower one for measuring discharge and the upper one for model exploration (Figure 1). The upper flume has a rectangular section measuring 16.2 m (length), 65 cm (width) and 66 cm (depth). The total length of the flume is divided into three parts: the inlet part, the working section, and the outlet part. Stones of different sizes were used at the entrance to the upper flume to damp flow disturbance carefully. The lower flume has the following dimensions: 99 cm (width), 100 cm (depth), and 18 m (length). This flume is provided with a pre-calibrated rectangular weir to measure the flow rate. The discharge varies from 15 l/s to 30 l/s.

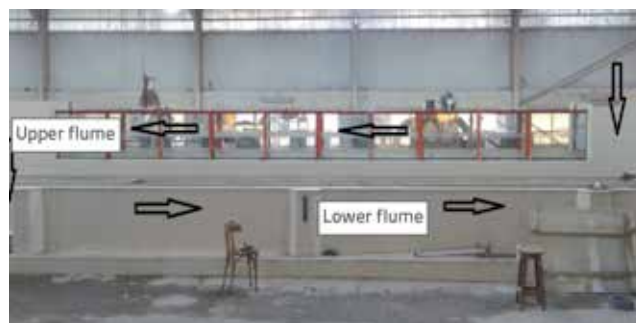


Figure 1. General view of laboratory apparatus and flow direction

	2x1	1x2	2x2
$w = 3.5, 4, 6, 9 \text{ cm}$ $l = 4, 6, 9, 10 \text{ cm}$	$(x, y)$ for different groups of piles cm, $w/L = 1$		
$w/l = 0.34, 0.43, 1, 2.25$	$(3.5, 3.5) - (7.0, 3.5) - (3.5, 10.5) - (10.5, 3.5) - (3.5, 7.0)$		$(9, 3) - (3, 3) - (3, 6) (3, 9) - (6, 3)$
$F_t = 0.2 \text{ to } 0.6$			

Figure 2. Arrangements of experimental models

The movable bed consists of uniform sand with a medium size of 1.4 mm and a fill flume with a depth of 0.12 m. The geometric standard deviation ( $\sigma_g$ ) is 1.28. The experimental work was conducted under clear-water conditions. For each test of the experimental program, the sand was levelled along the entire length of the flume using a wooden screed with the same width as the flume. The sand level was checked at random points with a point gauge. The flume was slowly filled with water to the required depth. The pump was then turned on, and its speed was increased slowly until the desired flow rate was achieved. Subsequently, the tailgate was adjusted to obtain the required water depth. At the end of the test, the pump was turned off, and the flume was drained slowly without disturbing the scour topography. A point gauge with 0.10-mm accuracy was used to map the bed topography and measure the water depth.

The tail water depth was varied ( $y_t = 8$  cm to 14 cm) to cover the range of Froude numbers ( $F = 0.20$  to 0.6). The total cross-sectional area of the piers in a group is equal to the area of one pier reference case. The width (3.5, 4, 6 and 9 cm),  $w$  (transversal direction of the channel), and length (4, 6, 9, and 10 cm),  $l$  (longitudinal direction of the channel), of the pier were changed to have the following  $w/l$  ratios (0.34, 0.43, 1.0 and 2.25). Various pier group arrangements are shown in Figure 2: one pier (reference case), triangular  $2 \times 1$  and  $1 \times 2$  (three piers), and  $2 \times 2$  (four piers) arrangements. The distances between piers in line (in the flow direction) and normal to flow direction were changed (i.e.  $x$  and  $y$ , Figure 2). The model width is less than 12 % of the channel width to avoid contraction effects [9]. The time for each experiment was 6 h, within which more than 85 % of the equilibrium scour depth was achieved on the basis of the preliminary experiments. Mia and Nago (2003) [23] and Yanmaz and Altinbilek (1991) [24] reported that most of the scour occurs during the first 3 or 4 hours of the test.

### 3. Numerical model

The SSIIIM model is a 3D software for simulating water and sediment movements. It was developed by Olsen in 2009 [25]. The computational fluid dynamics model is based on the finite volume method (FVM) and solves Navier–Stokes equations using the  $k$ - $\epsilon$  turbulence model. The eddy viscosity relationship can be calculated as

$$V_T = c_u \left( \frac{k}{\epsilon^2} \right) \quad (1)$$

Where  $k$  is the turbulence kinetic energy and is modelled by the following equation:

$$\frac{\partial k}{\partial t} + U_j \frac{\partial k}{\partial x_j} = \frac{\partial}{\partial x_j} \left( \frac{V_T}{\sigma_k} \frac{\partial k}{\partial x_j} \right) + V_T \frac{\partial U_j}{\partial x_i} \left( \frac{\partial U_j}{\partial x_i} + \frac{\partial U_i}{\partial x_j} \right) - \epsilon \quad (2)$$

The dissipation of  $k$  is assigned ( $\epsilon$ ) as

$$\frac{\partial \epsilon}{\partial t} + U_j \frac{\partial \epsilon}{\partial x_j} = \frac{\partial}{\partial x_j} \left( \frac{V_T}{\sigma_k} \frac{\partial \epsilon}{\partial x_j} \right) + C_{\epsilon 1} \frac{\epsilon}{k} P_k + C_{\epsilon 2} \frac{\epsilon^2}{k} \quad (3)$$

The " $C_{\epsilon 1,2}$ " coefficients are constant, and the default turbulence model in SSIIIM is  $k$ - $\epsilon$ .

The governing equations in numerical model for the non-compressible and constant flow can be modelled as follows:

$$\frac{\partial}{\partial x_j} (\rho U_j) = 0 \quad (4)$$

$$\frac{\partial}{\partial x_j} (\rho u_j u_i) = -\frac{\partial P}{\partial x_j} \delta_{ij} + \frac{\partial}{\partial x_j} \mu \left( \frac{\partial u_i}{\partial x_j} + \frac{\partial u_j}{\partial x_i} \right) + \frac{\partial}{\partial x_j} (-\overline{\rho u_i u_j}) \quad (5)$$

Equations 4 and 5 represent the continuity and momentum equations, respectively.  $U$  is the velocity component,  $\rho$  is the fluid density,  $P$  is the total pressure, and  $-\overline{\rho u_i u_j}$  is the Reynolds stress term that is evaluated using the turbulence model  $k$ - $\epsilon$ . Van Rijn (1987) [26] developed a formula to determine the equilibrium sediment concentration ( $C_{bed}$ ) close to the bed:

$$C_{bed} = 0.015 \frac{D^{0.3}}{a} \frac{\left[ \frac{\tau - \tau_c}{\tau_c} \right]^{1.5}}{\left[ \frac{(\rho_s - \rho_w) g}{\rho_w v^2} \right]^{0.1}} \quad (6)$$

In the equation (6),  $D$  is the sediment particle diameter,  $a$  is the reference level set equal to the roughness height,  $\tau$  and  $\tau_c$  are the bed shear stress and critical bed shear stress for movement of sediment particles according to Shield's diagram, respectively,  $\rho_w$  and  $\rho_s$  are the density of water and sediment respectively,  $\nu$  is the kinematic viscosity of water, and  $g$  is the gravitational acceleration. The bed load ( $q_b$ ) can be determined using Van Rijn 1987 [26] formula:

$$\frac{q_b}{D_{50}^{1.5} \sqrt{\frac{(\rho_s - \rho_w) g}{\rho_w}}} = 0.053 \frac{D_{50}^{0.3}}{D_{50}^{0.3}} \frac{\left[ \frac{\tau - \tau_c}{\tau_c} \right]^{1.5}}{\left[ \frac{(\rho_s - \rho_w) g}{\rho_w v^2} \right]^{0.1}} \quad (7)$$

where,  $D_{50}$  is the mean size of sediment.

The rough boundaries are modelled through the inclusion of the wall law, Schlichting, 1979 [27]:

$$\frac{U}{U_*} = K^{-1} \ln \left( \frac{30z}{k_s} \right) \quad (8)$$

where  $k_s$  is the roughness height,  $K$  is the von Karmen constant,  $U$  is the mean velocity,  $U_*$  is the shear velocity, and  $z$  is the height above the bed.

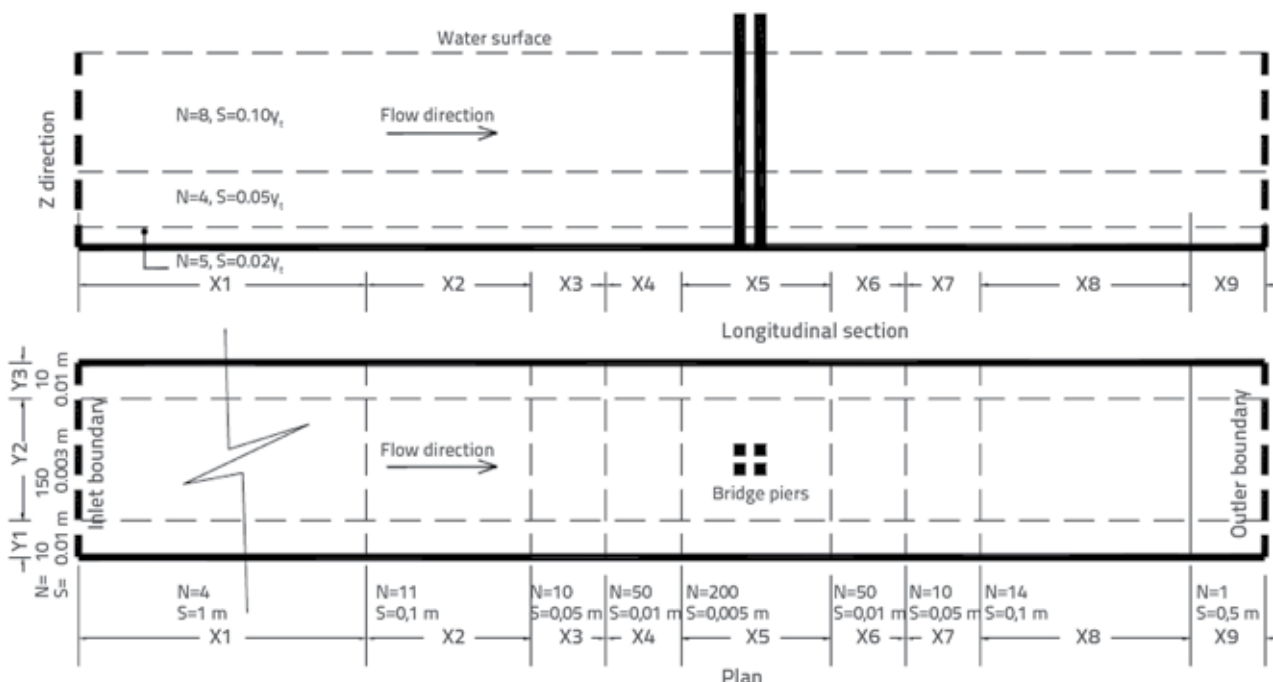


Figure 3. Layout of model grids

### 3.1. Geometry and properties of numerical model

A 3D-structured grid mesh with 350 elements in the X-direction, 170 elements in the Y-direction, and 17 elements in the Z-direction, was used in the CFD program (SSIIM), and the distribution of the grid lines of the mesh is presented in Figure 3. The figure shows that fine cells were used close to bridge piers to provide accurate simulation results, whereas coarser cells were employed away from the piers to optimise computational time. In the boundary conditions, the initial water level, flow rate and sediment size were defined as model inputs of the SSIIM. The zero gradient at the downstream boundary condition was applied to prevent instabilities in the model. A time step of 20 seconds was used. The bed changes were critically dependent on  $k_s$  in the wall law relation. The value of roughness height varied from  $D_{50}$  to  $100D_{50}$  [25]. After a trial-and-error procedure, a value of  $10D_{50}$  (0.014 m) for the roughness height was in good agreement with the bed changes in the experiment.

## 4. Analysis and discussions

### 4.1. One pier configuration

Here, the effect of varying width-length ratios of the pier on the scour formed at the one-pier case was investigated. The relative widths of pile ( $w/l$ ) are 0.34, 0.43, 1.0, and 2.25. The scour depth decreases with the relative width of the pile ( $w/l$ ) (Figure 4). The scour depth decreased by 32 % and 20 % for  $w/l = 0.34$  and 0.43, respectively. For the large value of  $w/l (= 2.25)$ , the local scour depth increased by 18 % compared with the reference pier case

( $w/l = 1.0$ ). The local scour around the pier was caused by the downflow of water at the upstream of the pier and the horseshoe vortex at the base of the pier. The increase in the relative pier width enhanced the concentration of the impinging downward velocity upstream the pier, thereby leading to large dimensions of scour holes at the bridge support. The longitudinal average time of velocity vectors for the typical cases of  $w/l = 1$  and 0.34 are presented in Figure 5. The downward velocity vectors impinge at the upstream pier, generating a scour hole upstream. In addition, wake vortices were generated downstream bridge pier, thereby forming a small scour hole. The power of horse shoe vortex was reduced for the smaller values of  $w/l (= 0.34)$ . The prediction equation for a single pier (HEC-18) by Richardson and Davis (2001) [13] was applied for typical cases of the present study, that is,  $w/l = 1$  and 2.25, Figure 4. The HEC-18 equation produced reliable results for the case of  $w/l = 1$  and overestimated results for the case of  $w/l = 2.25$ . Therefore, multiple linear regression was applied on the experimental data to propose an empirical equation, correlating the local scour depth with the width-length ratio ( $w/l$ ) and the Froude number ( $F_t = u/(gy_t)^{0.5}$ , where  $u$  is the average velocity,  $y_t$  is the tail water depth, and  $g$  is the gravitational acceleration), as follows:

$$d_s / y_t = -1,45 + 0,17 (w / l) + 2,65 F_t \tag{9}$$

The results predicted for the proposed equation were compared with the measured data (Figure 6). The coefficient of determination ( $R^2$ ) and the standard error for Equation (9) were 0.95 and 0.08, respectively. This equation expresses the measured data well.

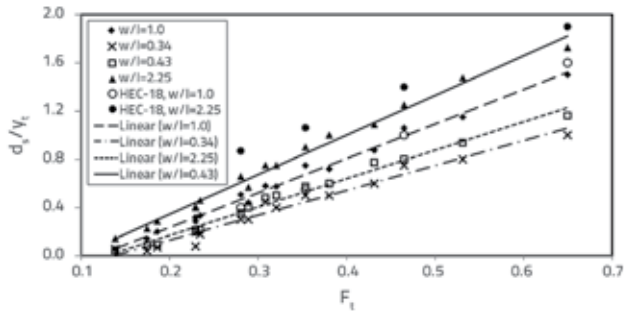


Figure 4. One pier case: Relationship between  $F_t$  and  $d_s/y_t$  for different  $w/l$

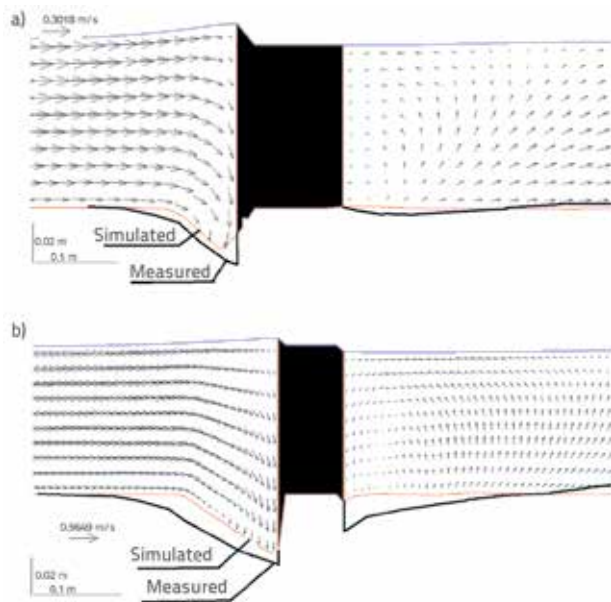


Figure 5. Longitudinal average time velocity for different ratios of  $w/l$  at  $F_t = 0.52$ , (Case of one pier)

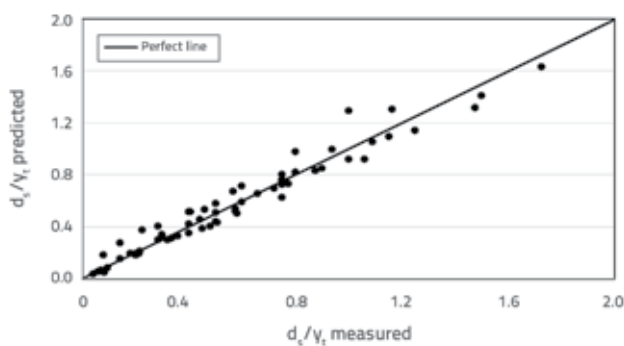


Figure 6. Predicted results of Eq. (9) versus measured data for different  $w/l$

### 4.2. Arrangements of pier groups

The effect of varying spaces between piers in different groups on local scour depth are investigated. Figure 2 shows the arrangements of piers in different groups. The relative distances

in the line of flow ( $x_o = x/(\text{side length of pier})$ ) and normal to the flow line direction ( $y_o = y/(\text{side length of pier})$ ), were changed for different experimental models (2x1, 1x2, and 2x2).

#### 4.2.1. Triangular 2x1 arrangements

The relationships between the Froude number ( $F_t$ ) and the relative scour depth ( $d_s/y_t$ ) for the  $2 \times 1$  case, and different spacing between piers ( $x_o$  and  $y_o$ ), are shown in Figure 7.

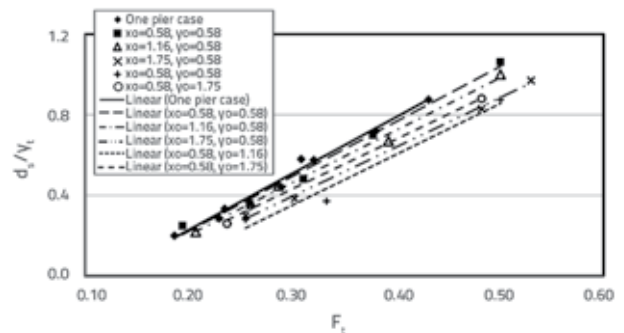


Figure 7. Relationship between  $F_t$  and  $d_s/y_t$  for case of 2x1 and different  $x_o$  and  $y_o$

All arrangement cases of the  $2 \times 1$  pier group produce small  $d_s/y_t$  values compared to that of the one bridge pier case. A slight effect of the spacing between piers on the scour formed at the bridge foundation for cases of  $x_o = 0.58$  and  $y_o = 0.58$  was observed. The time average velocity vectors of the last case show that a significant concentration of eddies between piers was generated, thus explaining the formation of high values of local scour depth (Figure 8.a). The vortices between piers decrease ( $x_o = 0.58, y_o = 1.16$ , Figure 8.c) as the relative vertical distance between piles ( $y_o$ ) increases. The horizontal velocity vectors formed downstream of the upstream piers impinge those generated upstream of the last pile. Thus, a reduction of the power of horseshoe vortices at the pier group was observed. For large values of  $y_o$  ( $= 1.75$ ), the interaction between piers is slightly low, and the local scour depth increased compared with that in the case of  $y_o = 1.16$ . For the pier spacing of  $y_o = 0.58$ , the local scour depth slightly decreases as  $x_o$  increases. The local scour depths for  $x_o = 0.58$  and  $1.16$  decrease by 3 % and 6 %, respectively. Figure 8.b presents the formation of vortices around piers for the case of  $x_o = 1.16$  and  $y_o = 0.58$ , indicating that the longer the distance of  $x_o$  shares to accumulate bundle of flow towards the downstream pier, the greater the increase in the scour depth. Finally, for the  $2 \times 1$  pier arrangements, the distance between piers normal with flow line ( $y_o$ ) is considered as a predominant factor affecting the local scour depth. The best distances between piles in the present arrangement are  $x_o = 0.58$  and  $y_o = 1.16$  at which the local scour depth is reduced by 30 %. A prediction equation was developed to estimate the maximum scour depth at the triangular arrangement of piers (2x1) as follows:

$$d_s / y_t = -1,45 + 0,3 (x_o/y_o)^{0,03} + 2,9 F_t^{0,5} \tag{10}$$

The above equation expresses the measured data quite adequately. The predicted and measured data are adequately distributed around the perfect line, as shown in Figure 9. The coefficient of determination and standard error amount to 94 % and 0.06, respectively.

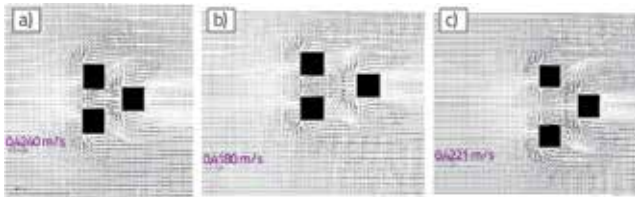


Figure 8. Average velocity vectors around piers away from bed by 0.01 of water depth for  $F_t = 0.50$ : a)  $x_o = 0,58, y_o = 0,58$ ; b)  $x_o = 1,16, y_o = 0,58$ ; c)  $x_o = 0,58, y_o = 1,16$

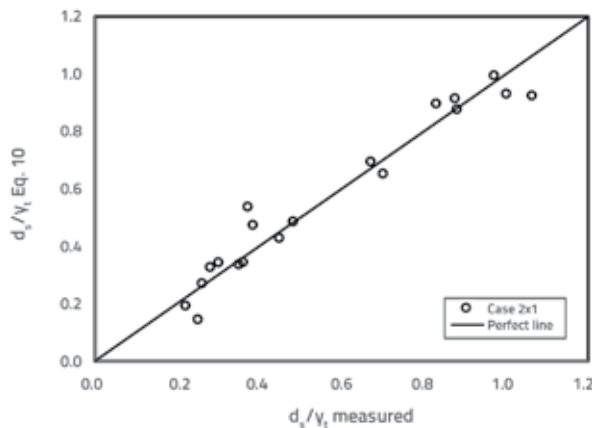


Figure 9. Measured versus predicted of Eq. (10) for case of 2x1 arrangements

#### 4.2.2. Triangular 1x2 arrangements

The relative scour depth versus the Froude number for the different cases of  $1 \times 2$  pier arrangements is presented in Figure 10. The small spacing between piers in line and normal to the flow direction, that is, ( $x_o = 0.58$ , and  $y_o = 0.58$ ), slightly reduces the scour depth by 2.5 % compared with the one bridge pile case. The scour depth decreases by 8 % and 20 % for  $x_o = 1.16$  and  $1.75$  at  $y_o = 0.58$ , respectively. In addition, the effect of changing of  $y_o$  on the local scour depth at  $x_o = 0.58$  is slightly low. The reduction percentages of scour at  $y_o = 0.58$  and  $1.16$  at  $x_o = 0.58$  were 2.5 % and 7 %, respectively. Velocity vectors around pier groups are shown in Figure 11. Clearly, strong vortices in-between piers were generated for small distance between piers, thereby producing more depths of scour than in the other large spaces between piers (Figure 11.a). Increasing the distance of  $x_o$  enhanced the upstream pier in a group arrangement as a sacrificial pile, and so the reduction in power of vortices upstream of the last piers was obtained, and a smaller local scour depth was generated (Figure 11.c). The increase in  $y_o$  (1.16) with  $x_o = 0.58$  permitted the velocity vectors to concentrate upstream of

each pier in a group (Figure 11.b). Vortices were generated, especially in front of downstream piers to form larger dimensions of scour holes between the three piers. The proposed equation for estimating the maximum scour depth for the case of ( $1 \times 2$ ) is:

$$d_s / y_t = -2,40 - 0,56 (x_o/y_o)^{0,05} + 4,6 F_t^{0,25} \tag{11}$$

The coefficient of determination and the standard error are 96 % and 0.051, respectively. Figure 12 presents values predicted in Equation (11) versus the measured data. Equation\_based predicted results are consistent with the experimental data.

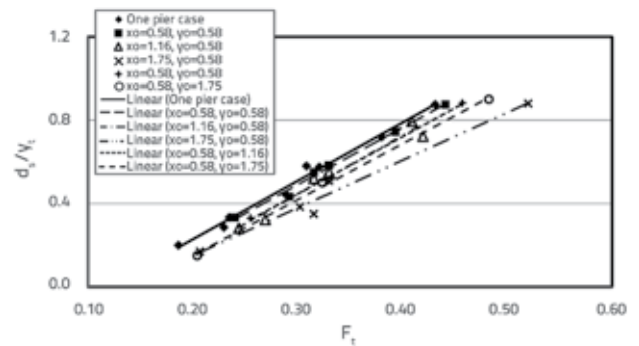


Figure 10. Relationship between  $F_t$  and  $d_s/y_t$  for case of 1x2 and different  $x_o$  and  $y_o$



Figure 11. Average velocity vectors around piles (Case of 1x2 arrangements) away from bed by 0.01 of water depth for  $F_t = 0.50$

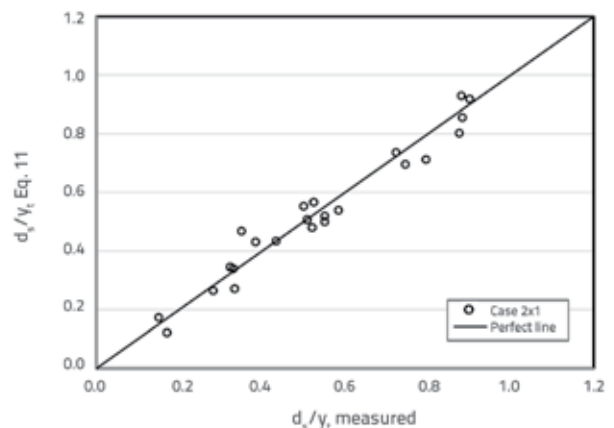


Figure 12. Measured versus predicted (Eq. (11)) for case of 1x2 arrangements

#### 4.2.3. Rectangular 2x2 arrangements

The relationship between the relative scour depth and the Froude number for various distances between piers in the  $2 \times 2$  group is shown in Figure 13. The pier arrangement shows that

by fixing the relative distance in the flow line direction ( $x_0 = 0.5$ ), the local scour depth decreases as the distance of  $y_0$  increases. The relative scour depth decreases by 8 %, 15 %, and 24 %, for the arrangements of  $y_0 = 0.5, 1.5$ , and  $1.0$ , respectively, at  $x_0 = 0.5$  compared with the one pier case. The velocity vectors around the piers are shown in Figure 14.

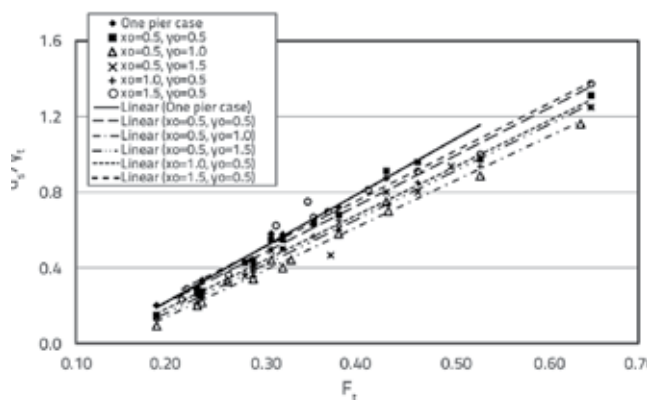


Figure 13. The relationship between  $F_t$  and  $d_s/y_t$  for case of 2x2 and different  $x_0$  and  $y_0$

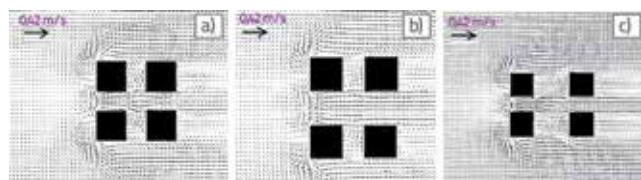


Figure 14. Average velocity vectors around piers (Case of 1x2 arrangements) away from bed by 0.01 of water depth for  $F_t = 0.50$ : a)  $x_0 = 0,5, y_0 = 0,5$ ; b)  $x_0 = 0,50, y_0 = 1,0$ ; c)  $x_0 = 1,5, y_0 = 0,50$

The small distances between piers in line and normal to flow directions generate more eddies in front and between pier groups compared with the larger distances between piers, especially for the case of  $x_0 = 0.5$  and  $y_0 = 1$  (Figure 14.a, 14.b). The present arrangement of piers shows that varying the normal distance

between piers with the flow direction is a predominant reason for reducing scour depth around piers rather than the distance in the flow line direction. Figure 14.c shows that the scour formed at  $x_0 = 1.5$  and  $y_0 = 0.5$  is exposed to large concentration of eddies in front and at the mid-zone area between piers, thereby generating a large scour depth at the group of piers. A statistical equation was proposed to determine the maximum scour depth for the pier arrangement of  $(2 \times 2)$  as follows:

$$d_s / y_t = -0,37 + 0,06 (x_0/y_0)^{0,5} + 2,45 F_t^{0,33} \quad (12)$$

The proposed equation correlates the relative scour depth with other independent parameters. The coefficient of determination and standard error are 95 % and 0.057, respectively. Equation (12) expresses the measured data adequately (Figure 15).

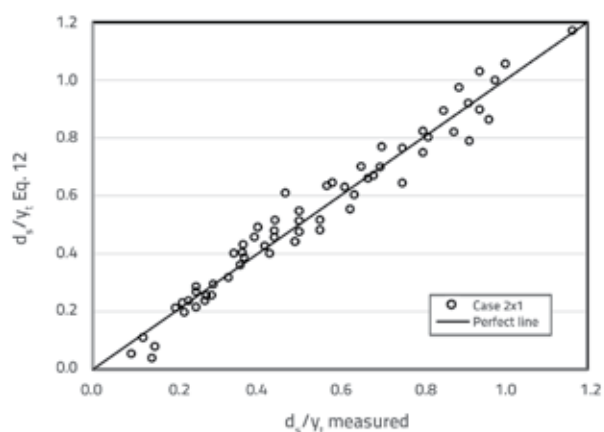


Figure 15. Measured versus predicted results of Eq. (12) for case of 2x2 arrangements

## 5. Verification of numerical model

Numerical results based on the SSIM model were verified using the experimental data for different pier group arrangements. A comparison between the simulated and observed scour depths is presented in Table 1. The average absolute error for the typical

Table 1. Comparison between simulated and observed scour depths

Model type	x [cm]	y [cm]	$y_t$ [cm]	Q [l/s]	Simulated scour [cm]	Observed scour [cm]	Absolute error = absolute (observed-simulated) / observed
Single pier	-	-	14	15	0.8	0.75	0.07
	-	-	14	20.1	2.8	2.9	0.03
	-	-	14	24	4	3.8	0.05
	-	-	14	30	7.1	7.4	0.04
1x2 pier group	3.5	3.5	10	20.6	5.5	5.8	0.05
	3.5	3.5	8	20.6	7	6.6	0.06
	3.5	3.5	12	20.6	4	3.8	0.05
	7	3.5	10.3	16.6	2.9	3.2	0.09
	7	3.5	7.3	16.6	5.8	6	0.03
		3.5	12.1	23.4	3.9	3.85	0.01

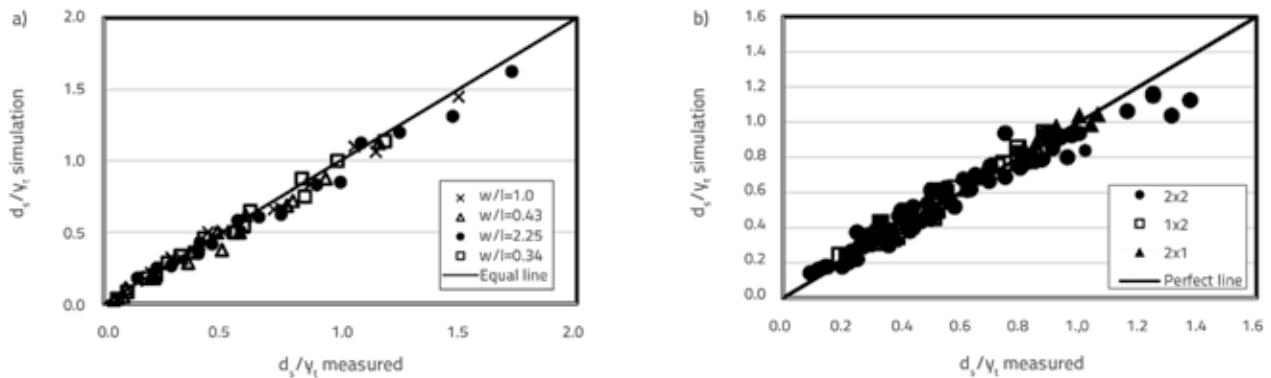


Figure 16. Verification of numerical model for different cases of a)  $w/l$  (relative widths of one pier case), and b) arrangements of pier groups

simulated cases (cases of one bridge pier and 1x2 pier group) is approximately 5%. These results indicate that the scour around bridge piers can be simulated using the SSIIM model. The relationship between the simulated results and the measured data for all studied cases is shown in Figure 16. In addition, the measured and simulated bed profiles for typical cases of  $w/l = 0.43$  and 1.0 are presented in Figure 5. The clear agreement between the numerical and measured data indicates that the SSIIM model can simulate the local scour depth generated at different arrangements of pier groups. The coefficient of determination and standard error for the simulated data are 97% and 0.04, respectively.

## 6. Conclusions

Experimental and numerical studies are carried out to investigate how the local scour depth is affected by varying the spacing between piers in line and normal to flow directions. The experimental models include, one pier, three piers (2x1 and 1x2) and four piers (2x2) arrangements. The computational fluid dynamics models, which are based on the finite volume method used to solve Navier-Stokes equations, were developed using

the SSIIM program. The following conclusions can be drawn from the results:

- The HEC-18 equation by Richardson and Davis, 2001 [13] produces a reliable prediction of local scour for  $w/l = 1$ , and overestimated predictions for other ratios of  $w/l$ .
- For the best arrangements of pier groups  $1 \times 2$ ,  $2 \times 1$  and  $2 \times 2$ , the local scour depths decreased by 20%, 30% and 24%, respectively, compared with that of the one pier case.
- The local scour depth is significantly affected by distance in the line of flow direction for the 1x2 pier group, whereas the normal spaces with the flow line direction affected the cases of 2x1 and 2x2 pier groups.
- The simulated results of the 3D CFD models obtained using the SSIIM program are consistent with the experimental data for various models.
- The results of the proposed empirical equations agree well with measured data.

## Acknowledgements

This research was carried out with the support of the deanship of scientific research - Jazan University.

## REFERENCES

- [1] Hunt, B.: Monitoring Scour at Critical Bridges, Washington, D.C, 2009.
- [2] Hamill, L.: Bridge hydraulics, London: E& FN Spon, 1999.
- [3] Melville, B.W., Coleman, S.E.: Bridge Scour. Water resources publications. Highlands Ranch, Colorado, 2000.
- [4] Briaud JL, Ting F., Chen, H.C., Gudavalli R., Perugu S., Wei G., Sricos.: Prediction of scour rate in cohesive soils at bridge piers. Journal of Geotechnical and Geoenvironmental Engineering, 125 (1999) 4, pp. 237-46.
- [5] Fischenich, J.C., Landers, M.: Computing Scour, Technical Note EMRRPSR-05, <http://el.erdc.usace.army.mil/elpubs>, 2000.
- [6] Lanca, R., Fael, C., Maia, R., Joao P. Pego, P.J.: Clear-water scour at pile groups. J. Hydraul. Eng., 139 (2013) 10, pp.1089 - 1098.
- [7] Bayram, A., Larson, M.: Analysis of scour around a group of vertical piles in the field, Journal of Waterway, Port, Coastal, and Ocean Engineering, 126 (2000) 4, pp.125-220.
- [8] Ettema, R.: Scour at Bridge Piers, Report No. 216, School of Engineering, Univ. of Auckland, Auckland, New Zealand, 1980.
- [9] Melville, B.W., Sutherland, A.J.: Design method for local scour at bridge piers, J. Hydraul. Eng., 114 (1988)10, pp. 1210-1226.

- [10] Dey, S., Bose, S.K., Sastry, G.N.: Clear-water scour at circular piers: a model, *J. Hydraul. Eng.*, 121 (1995) 12, pp. 869–876.
- [11] Kumar, V., Ranga Raju, K.G., Vittal, N.: Reduction of local scour around bridge piers using slot and collar, *J. Hydraul. Eng.*, 125 (1999) 12, pp.1302-1305
- [12] Mohamed, Y.A., Saleh, Y.K., Ali, A.M.: Experimental investigation of local scour around multi-vents bridge piers. *Alexandria Engineering Journal*, 54 (2015) 2, pp.197–203.
- [13] Richardson, E.V., Davis, S.R.: *Evaluating Scour at Bridges*, Hydraulic Engineering Circular No. 18, Federal Highway Administration, Washington, D.C, 2001.
- [14] Hannah, C.R.: *Scour at pile groups*, Research Report No. 28-3, Civil Engineering Department, University of Canterbury, Christchurch, New Zealand, 1978.
- [15] Ataie-Ashtiani, B., Beheshti, A.: Experimental investigation of clear-water local scour at pile groups, *J. Hydraul. Eng.*, 132 (2006) 10, pp.1100–1104.
- [16] Amini, A., Melville, B.W., Ali, T.M., Ghazali, A.H.: Clear-water local scour around pile groups in shallow-water flow, *J. Hydraul. Eng.*, 138 (2012) 2, pp. 177-185.
- [17] Moussa, Y.A., Atta, M.: Effect of Pile Arrangement on Local Scour Depth, *Proceedings of the 37<sup>th</sup> IAHR World Congress*, Kuala Lumpur, Malaysia, pp. 338-347, 2017.
- [18] Sumer, B.M., Bundgaard, K., Fredsøe, J.: *Global and Local Scour at Pile Groups*, *Proceedings of the 15<sup>th</sup> International Offshore and Polar Engineering Conference*, Seoul, Korea, pp.577-583, 2009.
- [19] Rashed-Hosseini, Amini, A.: Scour depth estimation methods around pile groups, *KSCE, Journal of Civil Engineering*, 19 (2015) 7, pp. 2144-2156.
- [20] Morales, R., Ettema, R.: Insights from depth-averaged numerical simulation of flow at bridge abutments in compound channels. Department of Civil and Architectural Engineering, University of Wyoming Laramie, WY 82071, 2011.
- [21] Mohamed, Y.A., Abdel-Aal, G.M., Nasr-Allah, T.H, Awad, A.S.: Experimental and theoretical investigations of scour at bridge abutment, *Journal of King Saud University- Engineering Sciences*, 28 (2016) 1, pp. 32–40
- [22] Nasr-Allah, T.H., Mohamed, Y.A, Abdel-Aal, G.M., Awad, A.S.: Experimental and numerical simulation of scour at bridge abutment provided with different arrangements of collars, *Alexandria Engineering Journal*, 55 (2016) 2, pp.1455–1463.
- [23] Mia, M., Nago, H.: Design method of time-dependent local scour at circular bridge pier, *Journal of Hydraulic Engineering*, 129 (2003) 6, pp. 420-427
- [24] Yanmaz, M., Altinbilek, H.D.: Study of time-dependent local scour around bridge piers, *Journal of Hydraulic Engineering*, 117 (1991) 10, pp.1247–1268.
- [25] Olsen, N.: *A three-dimensional numerical model for simulation of sediment movements in water intakes with multiblock option*. Department of Hydraulic and Environmental Engineering: the Norwegian University of Science and Technology, 2009.
- [26] Van Rijn, L.C.: *Mathematical Modeling Of Morphological Processes In The Case Of Suspended Sediment Transport*, Thesis, Delft Tech. Univ., Delft, The Netherlands, 1987.
- [27] Schlichting, H.: *Boundary-Layer Theory*, 7<sup>th</sup> edition. McGraw-Hill, New York, 1979.